NANO LETTERS

Letter

pubs.acs.org/NanoLett

Graphene Oxide-Based Carbon Interconnecting Layer for Polymer Tandem Solar Cells

Yonghua Chen,[†] Wei-Chun Lin,[†] Jun Liu,[‡] and Liming Dai*[,†]

[†]Center of Advanced Science and Engineering for Carbon (Case4Carbon), Department of Macromolecular Science and Engineering, Case School of Engineering, Case Western Reserve University, 10900 Euclid Avenue, Cleveland, Ohio 44106, United States

[‡]State Key Laboratory of Polymer Physics and Chemistry, Changchun Institute of Applied Chemistry, Chinese Academy of Sciences, Changchun 130022, People's Republic of China

S *Supporting Information*

ABSTRACT: Tandem polymer solar cells (PSCs), consisting of more than one (normally two) subcells connected by a charge recombination layer (i.e., interconnecting layer), hold great promise for enhancing the performance of PSCs. For an ideal tandem solar cell, the open circuit voltage (V_{oc}) equals to the sum of those of the subcells while keeping the short circuit current the same as the lower one, leading to an increased overall power conversion efficiency. The interconnecting layer plays an important role in regulating the tandem device performance. Here, we report that graphene oxide (GO)/GO-Cs (cesium neutralized GO) bilayer modified with ultrathin Al and MoO_3 can act as an efficient interconnecting layer in tandem PSCs to achieve a significantly increased V_{oc}, reaching almost 100% of the sum of the subcell V_{oc}s under standard AM 1.5 conditions.

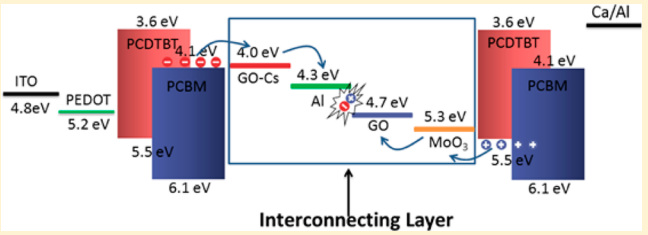

KEYWORDS: *Graphene oxide, interconnecting layer, polymer tandem solar cells, solution processability*

Polymer solar cells (PSCs) hold great potential to become a future energy source with lightweight, low cost, and superior large-area flexibility.[1−5] Tremendous efforts have been recently directed toward the development of high-power conversion efficiency (PCE) by developing novel photovoltaic active materials,[6−15] optimizing the active layer morphology,[5,16,17] and engineering interfacial structures.[18−25] Consequently, a new record-high PCE of 10.6% has been reported recently.[26] Along with the rapid progress in the material design and active layer engineering, PSCs with tandem (or stacked) architectures have attracted considerable interest due to their higher overall PCE.[3,27−36] Tandem PSCs have been devised by vertically stacking several (normally two) individual subcells connected by charge recombination layer (i.e., interconnecting layer), consisting of a hole-transporting layer/active layer/electron-transporting layer with the entire device having only two electrodes for charge collection. In a tandem solar cells of two subcells with stacking complementary absorption profiles, the open circuit voltage (V_{oc}) equals to the sum of those of the subcells while keeping the short circuit current the same as the lower one, leading to an increased overall PCE.

Functioning as both an internal anode and a cathode to facilitate an efficient electron and hole recombination for maximizing the V_{oc} and fill factor (FF), the interconnecting layer plays an important role in regulating the device performance. Generally speaking, an ideal interconnecting layer needs to possess an energy level matching with those of donor and acceptor (macro)molecules in the active layer, sufficient conductivity, high transparency, uniform coverage, and good chemical stability. For solution-processable interconnecting materials, they are also required to be robust enough to avoid any damage by the rear cell or damage caused by the interconnecting layer to the front cell during the processing process. Although many materials cannot meet the above stringent requirements, several interconnecting layers, including TiO_x/poly(3,4-ethylenedioxythiophene):poly(styrenesulfonate) (PEDOT:PSS),[3] ZnO/PEDOT:PSS,[30] MoO_3/Al/ZnO,[32] Al/TiO_2/PEDOT:PSS,[36] LiF/Al/Au/PEDOT:PSS,[37] LiF/Al/MoO_3,[38] and MoO_3/Ag/Al/Ca,[39] have recently been demonstrated to be useful in tandem solar cells. More recently, graphene oxide (GO) based interconnecting layers, such as ZnO/GO:PEDOT:PSS[34] and ZnO/GO:SWNTs,[31] have also been reported, indicating the potential application of GO-based materials as the interconnecting layer to replace PEDOT:PSS. Because of the low conductivity of GO, however, certain highly conductive materials (e.g., PEDOT:PSS, SWNTs) have to be blended into the GO interconnecting layer, which complicated the device fabrication and limited the V_{oc} of tandem cells to be only ~80% of the sum of the subcells. It remains a big challenge to design GO-based materials with controlled electronic properties for tandem solar devices with a high overall V_{oc}, and hence a high PCE.

Very recently, we have found that simple charge neutralization of the −COOH groups in GO with Cs_2CO_3 could tune the

Received: December 13, 2013
Revised: February 1, 2014

   dx.doi.org/10.1021/nl4046284 | *Nano Lett.* XXXX, XXX, XXX−XXX

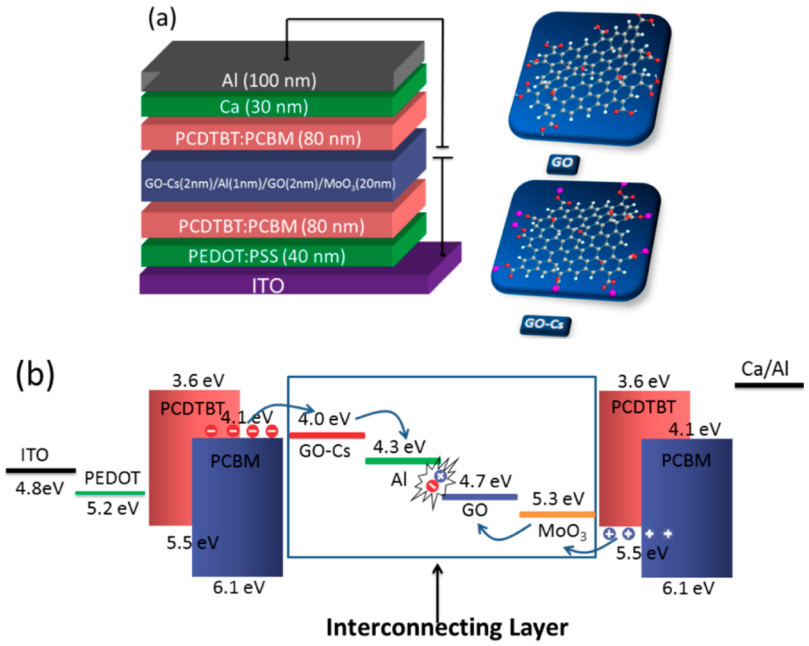

Figure 1. Device structure and energy levels of the polymer tandem solar cells. (a) Schematic of the tandem device structure in which a GO-Cs/Al/GO/MoO_3 interconnecting layer was employed. The final device structure is ITO/PEDOT:PSS (40 nm)/PCDTBT:PCBM (1:4, 80 nm)/GO-Cs (2 nm)/Al (1 nm)/GO (2 nm)/MoO_3 (20 nm)/PCDTBT:PCBM (1:4, 80 nm)/Ca (30 nm)/Al (100 nm). Top right: schematic representations of the chemical structures for the GO and GO-Cs used in the study. The white, red, and pink dots represent C, O, and Cs atoms, respectively. (b) Schematic energy-level diagram for the various layers of the optimized tandem device.

electronic structure of GO, and the resultant cesium-neutralized GO (GO-Cs) can act as an efficient electron extraction layer in polymer solar cells.[18] By replacing the periphery −COOH groups of GO with −COOCs groups via the charge neutralization, the work function of a GO-Cs modified Al substrate can be reduced to 4.0 eV, matching well with the lowest unoccupied molecular orbital (LUMO) level of [6,6]-phenyl-C61-butyric acid methyl ester (PCBM) for an efficient electron-extraction. Moreover, the GO-Cs can be well dissolved into ethanol, making the multilayer solution-processing feasible.

In the present study, we developed a GO-based carbon interconnecting layer consisting of GO-Cs/GO bilayer modified with ultrathin Al and MoO_3. The relatively weak light absorption characteristic of GO and GO-Cs, together with their good solution-processability for ultrathin film formation (*ca.* 2 nm), facilitates largely light transmission through the interconnecting layer to the rear cell. By careful design of the energy level alignment within the GO/GO-Cs interconnecting layer, efficient charge carrier collection from the subcells and charge recombination within the interconnecting layer were achieved. As a result, the tandem cells fabricated with the GO-Cs/GO-based interconnecting layer exhibited a significantly increased V_{oc} reaching ~100% of the sum of the subcell V_{oc}s, suggesting a successful serial connection of subcells. The PCE of 3.91% obtained from our tandem solar cell is 1.34 times that of the subcell (2.92%). Clearly, an effective connection between polymer subcells can be realized by GO-based interconnecting layers.

Figure 1a,b shows the device structure and energy levels of the polymer tandem solar cell, respectively. The active layer of both subcells consisted of a blend of poly [*N*-9′-heptadecanyl-2,7-carbazole-alt-5,5-(4′,7′-di-2-thienyl-2′,1′,3′-benzothiadiazole)] (PCDTBT)[40] as a polymeric electron donor and PCBM as an electron acceptor, which were connected by a GO-Cs/Al/GO/MoO_3 composite interconnecting layer. Although polymers with complementary absorption capabilities are needed for tandem solar cells to show a high PCE, the key index of successful tandem structure is the value of V_{oc}, which ideally should be the sum of the values of the individual subcells.

Figure 2 shows the current density−voltage (J−V) characteristics of tandem solar cells with different interconnecting layer

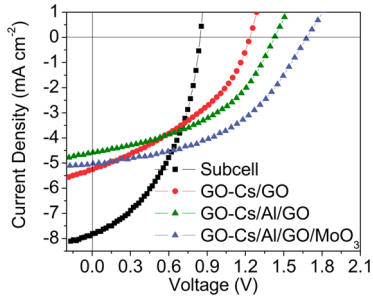

Figure 2. J−V characteristics of the subcell and tandem PSCs with different interconnecting layers under illumination of a solar simulator (100 mW cm^{-2}).

combinations under illumination of a Newport Oriel sol 2A solar simulator (300 W, 100 mW cm^{-2}). Table 1 summarizes the performance characteristics for all devices. As can be seen in Table 1 and Figure 2, the subcell with the structure of ITO/PEDOT:PSS (40 nm)/PCDTBT:PCBM (80 nm)/Ca (30 nm)/Al (100 nm) showed a V_{oc} of 0.85 V, J_{sc} of 7.82 mA cm^{-2}, FF of 0.44, and PCE of 2.92% in a good consistence with the report data.[41] The corresponding data for the tandem PSCs changed significantly with the variation of interconnecting layers, indicating that the interlayer plays a critical role in controlling the device performance through the charge recombination process. The tandem device with a GO-Cs/GO interlayer exhibited a V_{oc} of 1.23 V, J_{sc} of 5.26 mA cm^{-2}, FF

dx.doi.org/10.1021/nl4046284 | *Nano Lett.* XXXX, XXX, XXX−XXX

Table 1. Summary of $J-V$ Characteristics of the Subcell and Tandem Device with Different Interconnecting Layers (ICLs)

ICL	V_{oc} (V)	J_{sc} (mA cm^{-2})	FF	PCE (%)
subcell	0.85	7.82	0.44	2.92
GO-Cs/GO	1.23	5.26	0.38	2.46
GO-Cs/Al/GO	1.43	4.59	0.45	2.95
GO-Cs/Al/GO/MoO_3	1.69	5.03	0.46	3.91
Al/GO/MoO_3	1.56	4.95	0.43	3.32
GO-Cs/Al/MoO_3	1.60	4.57	0.40	2.92
Al/MoO_3	1.22	4.84	0.44	2.60

of 0.38, and PCE of 2.5%. Although the subcells were well separated by the GO-Cs/GO bilayer since the V_{oc} of the tandem PSC reached 72% of the sum of the subcell V_{oc}s (1.7 V), they are not electrically connected fully in series as reflected by the relatively low FF (0.38) and PCE (2.46%).[42] This could be attributed to the low conductivity of 3.8×10^{-3} and 5.0×10^{-3} S/m for GO and GO-Cs, respectively,[18] significant lower than PEDOT:PSS of typical 0.1 S/m. Moreover, the large energy gap between GO (4.7 eV) and GO-Cs (4.0 eV) limited the efficient charge recombination. A perfect interconnecting layer should efficiently collect electrons from one cell and holes from the other, and act as an efficient recombination zone for them without potential loss. When an ultrathin Al (~1 nm) film was inserted at the interface between the GO and GO-Cs layer, V_{oc} of the tandem device significantly increased from 1.23 to 1.43 V, which is 84% of the sum of the subcell V_{oc} (1.7 V). The FF also increased to 0.45, which is slightly higher than that of the subcell (0.44), leading to an increase in the PCE from 2.46% to 2.95%. Two functions of the ultrathin Al could be envisioned: (1) the work function of Al (~4.3 eV) matched well with those of the GO and GO-Cs to facilitate charge recombination, and (2) cesium salts, such as Cs_2CO_3 and CsF, have been reported to lower work function of Al cathode due to the formation of Cs−O−Al structure,[43] while the similar Cs−O−Al structure formation could also work for the GO-Cs to improve charge extraction from the active layer. As seen in Supporting Information Figure S1, the device performance also changed with the thickness of Al, lower V_{oc} and J_{sc} values for the thicker Al layers, which are presumably to have lower optical transparencies.

The fact that the V_{oc} of the tandem device with the GO-Cs/Al/GO interconnecting layer is not the sum of those of the two subcells indicates that some energy loss still exists because of the large energy gap between GO (4.7 eV) and the HOMO of PCDTBT (5.5 eV). In view of the energy level of 5.3 eV for MoO_3,[44] we devised a tandem device with the interconnecting GO-Cs/Al/GO layer further modified by MoO_3 (20 nm) to match the energy gap between GO and PCDTBT:PCBM active layer (Figure 1), which showed a significantly increased V_{oc} from 1.43 to 1.69 V (Table 1). The resultant V_{oc} for the tandem solar cell is approximately the sum of the V_{oc}s of the individual cells, indicating that the two subcells have indeed been electrically connected completely in series by the GO-Cs/Al/GO/MoO_3 interconnecting layer. The overall PCE reached to 3.91% (more than 34% increasement from the subcell), though the J_{sc} of the tandem device (5.03 mA cm^{-2}) was still lower than that of the subcell. Because two identical subcells were used in our tandem device, the optical absorption of the rear cell was inevitably limited by the optical absorption of the front cell, which led to a decrease in J_{sc} of the tandem devices.

The remarkable improvement in PCE was a result of the simultaneously enhanced V_{oc} (1.69 V) and FF (0.46), which in turn indicate that the GO-based interconnecting layer has made an excellent electrical connection through the ultrathin Al and MoO_3 modification to provide an efficient recombination region for electrons and holes generated from the front and rear cells, respectively. A histogram of the values of efficiencies and V_{oc}s for 29 sample devices using GO-Cs/Al/GO/MoO_3 as the interconnecting layer is presented in Supporting Information, Figure S2, which shows good reproducibility of the efficiency and ~100% sum of V_{oc}s. Furthermore, the GO-Cs/Al/GO/MoO_3 interconnecting layer exhibited a good transmission (Supporting Information, Figure S3), which is higher than 90% in the whole solar spectrum. Like the aforementioned thickness-dependence of the Al layer, however, the J_{sc} and FF were also influenced by the thickness of MoO_3 (Supporting Information, Figure S4).

To further investigate the photovoltaic parameters of tandem devices with different interconnecting layer combinations, we performed the electrical impedance spectrum measurements,[42,45,46] which enabled us to monitor the specific electrical properties of the interfaces that cannot be determined by direct-current measurements.[47] Figure 3 shows the Cole−Cole

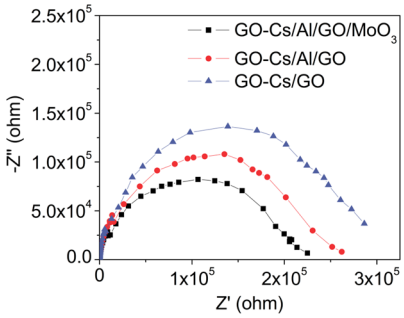

Figure 3. Impedance spectra of the tandem devices with different interconnecting layers in the dark.

plot (the imaginary resistance Z'' over the real resistance Z') of the tandem solar cells with different interconnecting layers in the dark, which revealed that the resistance of the interconnecting layer decreased in the order of GO-Cs/GO, GO-Cs/Al/GO, and GO-Cs/Al/GO/MoO_3. This is consistent to the concomitant decrease in the conductivity of the interconnecting layer with modification by Al and MoO_3, leading to the most efficient charge extraction and the electron−hole recombination for the GO-Cs/Al/GO/MoO_3 interconnecting layer.

The important role of GO and GO-Cs in the GO-Cs/Al/GO/MoO_3 interconnecting layer can be seen in Figure 4, which shows relatively low V_{oc} for the tandem devices using an interconnecting layer without GO-Cs, GO, or both. In these cases, the FFs are also much lower than that of the device with the GO-Cs/Al/GO/MoO_3 interconnecting layer (0.46). These results indicate that the use of the GO/MoO_3 bilayer as a hole transporting layer has significantly increased the FF in the polymer solar cells with respect to the GO or MoO_3 single layer.[48] The excellent electron-blocking ability of the GO layer allowed the interconnecting layer to efficiently block the current leakage and promote V_{oc} and FF in the tandem devices. This, together with the favorable energy matching to the LUMO level of PCBM for efficient electron extraction by the

dx.doi.org/10.1021/nl4046284 | Nano Lett. XXXX, XXX, XXX−XXX

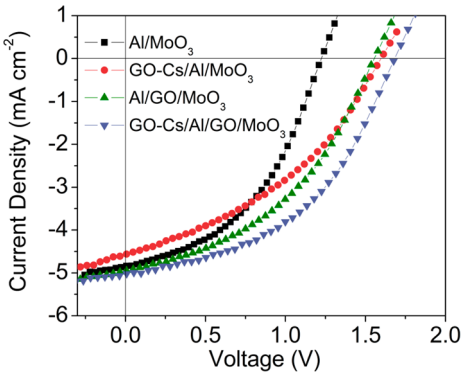

Figure 4. *J*–*V* characteristics of tandem cells based on interconnecting layer without GO-Cs or GO or both under illumination of a solar simulator (100 mW cm^{-2}).

Al-modified GO-Cs (Figure 1b), makes GO-Cs/Al/GO/MoO_3 an ideal interconnecting layer. However, possible contribution to the enhanced V_{oc} by surface doping the active layer with GO in the interconnecting layer cannot be ruled out.[18]

In summary, we have designed and fabricated tandem polymer solar cells using GO-based interconnecting layers and investigated the effects of interconnecting layer combinations on the device performance. For the first time, our results indicated that the GO-based interconnecting layer modified by ultrathin Al and MoO_3 could provide an efficient recombination region for electrons and holes generated from the front and rear cells due to excellent energy level matches for efficient charge transport and recombination. The power conversion efficiency of the optimized tandem solar cells exhibited a maximum PCE of 3.91% and V_{oc} of 1.69 V, reaching to ~100% of the sum of V_{oc}s of the subcells. Our results from the prototype devices indicate that graphene materials are very promising for applications as the interconnecting layer in tandem polymer solar cells.

Methods. *Device Fabrication and Measurements.* ITO glass substrates were cleaned sequentially with detergent, deionized water, acetone, and iso-propanol, followed by drying with N_2 flow and UV-ozone treatment for 15 min. The PEDOT:PSS was spin-coated from the solution (Al4083 from H. C. Starck) at 5000 rpm for 40 s, followed by heating at 140 °C for 10 min. Then, the active layer was spin-coated in an Ar-filled glovebox from the solution of PCDTBT:PCBM = 1:4 in o-dichlorobenzene (10 mg mL^{-1}) at 600 rpm for 60 s, followed by thermal annealing at 100 °C for 40 min. After spin-coating active layer, the device was transferred to outside from glovebox. GO-Cs was spin-coated from its H_2O/ethanol = 1:3 (0.5 mg mL^{-1}) solution at 2000 rpm for 60 s, followed by heating at 100 °C for 10 min. After spin-coating GO-Cs, the device was transferred to evaporator in the glovebox. After evaporating the ultrathin Al, GO was spin-coated from its dimethylformamide (0.5 mg mL^{-1}) solution at 2000 rpm for 60 s, followed by heating at 100 °C for 10 min. Then, a MoO_3 layer was deposited on top of GO by evaporation. After that, the second active layer was spin-coated. Finally, the device was transferred to the evaporator for deposition of Ca (30 nm) and Al (100 nm) by thermal evaporation at a pressure of 10^{-7} Torr. The area of each device is 0.12 cm^2, as determined by the overlap of the ITO and the evaporated Al. All the devices were tested in an Ar-filled glovebox using a Keithley 2400 source meter and a Newport Oriel sol 2A solar simulator (300 W). The light intensity was calibrated to be 100 mW cm^{-2} using a calibrated Si solar cell and a KG5 color filter. The device parameters were obtained from the current–voltage curves of the devices under illumination.

■ ASSOCIATED CONTENT

Ⓢ Supporting Information

Tandem device performance using GO-Cs/Al/GO as the interconnecting layers with different Al thicknesses and using GO-Cs/Al/GO/MoO_3 as the interconnecting layer with different MoO_3 thicknesses. A histogram of tandem solar cell efficiencies and open circuit voltages for 29 samples using GO-Cs/Al/GO/MoO_3 as the interconnecting layer. A typical transmission spectrum of the GO-Cs/Al/GO/MoO_3 interconnecting layer. This material is available free of charge via the Internet at http://pubs.acs.org.

■ AUTHOR INFORMATION

Corresponding Author

*E-mail: liming.dai@case.edu.

Notes

The authors declare no competing financial interest.

■ ACKNOWLEDGMENTS

The authors are very grateful for the financial support from AFOSR (FA9550-12-1-0069) under the Polymer Chemistry Task in the Directorate of Chemistry and Life Sciences (Dr. Charles Lee, program Manager).

■ REFERENCES

(1) Yu, G.; Gao, J.; Hummelen, J. C.; Wudl, F.; Heeger, A. J. *Science* **1995**, *270* (5243), 1789–1791.
(2) Li, G.; Zhu, R.; Yang, Y. *Nat. Photonics* **2012**, *6* (3), 153–161.
(3) Dou, L. T.; You, J. B.; Yang, J.; Chen, C. C.; He, Y. J.; Murase, S.; Moriarty, T.; Emery, K.; Li, G.; Yang, Y. *Nat. Photonics* **2012**, *6* (3), 180–185.
(4) He, Z. C.; Zhong, C. M.; Su, S. J.; Xu, M.; Wu, H. B.; Cao, Y. *Nat. Photonics* **2012**, *6* (9), 591–595.
(5) Li, G.; Shrotriya, V.; Huang, J. S.; Yao, Y.; Moriarty, T.; Emery, K.; Yang, Y. *Nat. Mater.* **2005**, *4* (11), 864–868.
(6) Zhao, G. J.; He, Y. J.; Li, Y. F. *Adv. Mater.* **2010**, *22* (39), 4355–4358.
(7) Inganas, O.; Zhang, F. L.; Andersson, M. R. *Acc. Chem. Res.* **2009**, *42* (11), 1731–1739.
(8) Liang, Y. Y.; Feng, D. Q.; Wu, Y.; Tsai, S. T.; Li, G.; Ray, C.; Yu, L. P. *J. Am. Chem. Soc.* **2009**, *131* (22), 7792–7799.
(9) Bijleveld, J. C.; Gevaerts, V. S.; Di Nuzzo, D.; Turbiez, M.; Mathijssen, S. G. J.; de Leeuw, D. M.; Wienk, M. M.; Janssen, R. A. J. *Adv. Mater.* **2010**, *22* (35), E242–E246.
(10) Piliego, C.; Holcombe, T. W.; Douglas, J. D.; Woo, C. H.; Beaujuge, P. M.; Frechet, J. M. J. *J. Am. Chem. Soc.* **2010**, *132* (22), 7595–7597.
(11) Amb, C. M.; Chen, S.; Graham, K. R.; Subbiah, J.; Small, C. E.; So, F.; Reynolds, J. R. *J. Am. Chem. Soc.* **2011**, *133* (26), 10062–10065.
(12) Huo, L. J.; Zhang, S. Q.; Guo, X.; Xu, F.; Li, Y. F.; Hou, J. H. *Angew. Chem., Int. Ed.* **2011**, *50* (41), 9697–9702.
(13) Huang, Y.; Guo, X.; Liu, F.; Huo, L. J.; Chen, Y. N.; Russell, T. P.; Han, C. C.; Li, Y. F.; Hou, J. H. *Adv. Mater.* **2012**, *24* (25), 3383–3389.
(14) Li, Y. F. *Acc. Chem. Res.* **2012**, *45* (5), 723–733.
(15) Liu, J.; Choi, H.; Kim, J. Y.; Bailey, C.; Durstock, M.; Dai, L. M. *Adv. Mater.* **2012**, *24* (4), 538–542.
(16) Peet, J.; Kim, J. Y.; Coates, N. E.; Ma, W. L.; Moses, D.; Heeger, A. J.; Bazan, G. C. *Nat. Mater.* **2007**, *6* (7), 497–500.
(17) Ma, W. L.; Yang, C. Y.; Gong, X.; Lee, K.; Heeger, A. J. *Adv. Funct. Mater.* **2005**, *15* (10), 1617–1622.

dx.doi.org/10.1021/nl4046284 | *Nano Lett.* XXXX, XXX, XXX–XXX

(18) Liu, J.; Xue, Y. H.; Gao, Y. X.; Yu, D. S.; Durstock, M.; Dai, L. M. *Adv. Mater.* **2012**, *24* (17), 2228−2233.
(19) Murase, S.; Yang, Y. *Adv. Mater.* **2012**, *24* (18), 2459−2462.
(20) Irwin, M. D.; Buchholz, B.; Hains, A. W.; Chang, R. P. H.; Marks, T. J. *Proc. Natl. Acad. Sci. U.S.A.* **2008**, *105* (8), 2783−2787.
(21) Yip, H. L.; Jen, A. K. Y. *Energ. Environ. Sci.* **2012**, *5* (3), 5994−6011.
(22) You, J. B.; Chen, C. C.; Dou, L. T.; Murase, S.; Duan, H. S.; Hawks, S. A.; Xu, T.; Son, H. J.; Yu, L. P.; Li, G.; Yang, Y. *Adv. Mater.* **2012**, *24* (38), 5267−5272.
(23) O'Malley, K. M.; Li, C. Z.; Yip, H. L.; Jen, A. K. Y. *Adv. Energy. Mater.* **2012**, *2* (1), 82−86.
(24) Zhou, Y. H.; Fuentes-Hernandez, C.; Shim, J.; Meyer, J.; Giordano, A. J.; Li, H.; Winget, P.; Papadopoulos, T.; Cheun, H.; Kim, J.; Fenoll, M.; Dindar, A.; Haske, W.; Najafabadi, E.; Khan, T. M.; Sojoudi, H.; Barlow, S.; Graham, S.; Bredas, J. L.; Marder, S. R.; Kahn, A.; Kippelen, B. *Science* **2012**, *336* (6079), 327−332.
(25) Kim, J.; Tung, V. C.; Huang, J. X. *Adv. Energy. Mater.* **2011**, *1* (6), 1052−1057.
(26) You, J. B.; Dou, L. T.; Yoshimura, K.; Kato, T.; Ohya, K.; Moriarty, T.; Emery, K.; Chen, C. C.; Gao, J.; Li, G.; Yang, Y. *Nat. Commun.* **2013**, *4*, 1446−1456.
(27) Ameri, T.; Li, N.; Brabec, C. J. *Energ. Environ. Sci.* **2013**, *6* (8), 2390−2413.
(28) Kim, J. Y.; Lee, K.; Coates, N. E.; Moses, D.; Nguyen, T. Q.; Dante, M.; Heeger, A. J. *Science* **2007**, *317* (5835), 222−225.
(29) Gilot, J.; Wienk, M. M.; Janssen, R. A. J. *Adv. Mater.* **2010**, *22* (8), E67−E71.
(30) Yang, J.; Zhu, R.; Hong, Z. R.; He, Y. J.; Kumar, A.; Li, Y. F.; Yang, Y. *Adv. Mater.* **2011**, *23* (30), 3465−3470.
(31) Tung, V. C.; Kim, J.; Huang, J. X. *Adv. Energy. Mater.* **2012**, *2* (3), 299−303.
(32) Chou, C. H.; Kwan, W. L.; Hong, Z. R.; Chen, L. M.; Yang, Y. *Adv. Mater.* **2011**, *23* (10), 1282−1286.
(33) Zhou, Y. H.; Fuentes-Hernandez, C.; Shim, J. W.; Khan, T. M.; Kippelen, B. *Energ. Environ. Sci.* **2012**, *5* (12), 9827−9832.
(34) Tung, V. C.; Kim, J.; Cote, L. J.; Huang, J. X. *J. Am. Chem. Soc.* **2011**, *133* (24), 9262−9265.
(35) Li, W. W.; Furlan, A.; Hendriks, K. H.; Wienk, M. M.; Janssen, R. A. J. *J. Am. Chem. Soc.* **2013**, *135* (15), 5529−5532.
(36) Sista, S.; Park, M. H.; Hong, Z. R.; Wu, Y.; Hou, J. H.; Kwan, W. L.; Li, G.; Yang, Y. *Adv. Mater.* **2010**, *22* (3), 380−383.
(37) Hadipour, A.; de Boer, B.; Wildeman, J.; Kooistra, F. B.; Hummelen, J. C.; Turbiez, M. G. R.; Wienk, M. M.; Janssen, R. A. J.; Blom, P. W. M. *Adv. Funct. Mater.* **2006**, *16* (14), 1897−1903.
(38) Zhao, D. W.; Sun, X. W.; Jiang, C. Y.; Kyaw, A. K. K.; Lo, G. Q.; Kwong, D. L. *Appl. Phys. Lett.* **2008**, *93* (8), 083305.
(39) Zhao, D. W.; Ke, L.; Li, Y.; Tan, S. T.; Kyaw, A. K. K.; Demir, H. V.; Sun, X. W.; Carroll, D. L.; Lo, G. Q.; Kwong, D. L. *Sol. Energy Mater. Sol. Cells* **2011**, *95* (3), 921−926.
(40) Park, S. H.; Roy, A.; Beaupre, S.; Cho, S.; Coates, N.; Moon, J. S.; Moses, D.; Leclerc, M.; Lee, K.; Heeger, A. J. *Nat. Photonics.* **2009**, *3* (5), 297−302.
(41) Etzold, F.; Howard, I. A.; Mauer, R.; Meister, M.; Kim, T. D.; Lee, K. S.; Baek, N. S.; Laquai, F. *J. Am. Chem. Soc.* **2011**, *133* (24), 9469−9479.
(42) Seo, J. H.; Kim, D. H.; Kwon, S. H.; Song, M.; Choi, M. S.; Ryu, S. Y.; Lee, H. W.; Park, Y. C.; Kwon, J. D.; Nam, K. S.; Jeong, Y.; Kang, J. W.; Kim, C. S. *Adv. Mater.* **2012**, *24* (33), 4523−4527.
(43) Huang, J. S.; Xu, Z.; Yang, Y. *Adv. Funct. Mater.* **2007**, *17* (12), 1966−1973.
(44) You, H.; Dai, Y. F.; Zhang, Z. Q.; Ma, D. G. *J. Appl. Phys.* **2007**, *101* (2), 026105.
(45) Ecker, B.; Egelhaaf, H. J.; Steim, R.; Parisi, J.; von Hauff, E. *J. Phys. Chem. C* **2012**, *116* (31), 16333−16337.
(46) Ecker, B.; Posdorfer, J.; von Hauff, E. *Sol. Energy Mater. Sol. Cells* **2013**, *116*, 176−181.
(47) Jo, S. J.; Kim, C. S.; Kim, J. B.; Ryu, S. Y.; Noh, J. H.; Baik, H. K.; Kim, Y. S.; Lee, S. J. *J. Appl. Phys.* **2008**, *103* (11), 114502.
(48) Chao, Y.-H.; Wu, J.-S.; Wu, C.-E.; Jheng, J.-F.; Wang, C.-L.; Hsu, C.-S. *Adv. Energy. Mater.* **2013**, *10* (3), 1279−1285.

NOTE ADDED AFTER ASAP PUBLICATION

This article was published ASAP on February 17, 2014. Several values in the last column of Table 1 have been changed. The correct version was published on February 18, 2014.

dx.doi.org/10.1021/nl4046284 | *Nano Lett.* XXXX, XXX, XXX−XXX